DOI: 10.5665/SLEEP.1290

Fast and Slow Spindles during the Sleep Slow Oscillation: Disparate Coalescence and Engagement in Memory Processing

Matthias Mölle, PhD[1]; Til O. Bergmann, PhD[2]; Lisa Marshall, PhD[1]; Jan Born, PhD[1,3]

[1]Department of Neuroendocrinology, University of Lübeck, Lübeck, Germany; [2]Department of Neurology, Schleswig-Holstein University Hospital, Kiel, Germany; [3]Department of Medical Psychology and Behavioral Neurobiology, University of Tübingen, Germany

Study Objectives: Thalamo-cortical spindles driven by the up-state of neocortical slow (< 1 Hz) oscillations (SOs) represent a candidate mechanism of memory consolidation during sleep. We examined interactions between SOs and spindles in human slow wave sleep, focusing on the presumed existence of 2 kinds of spindles, i.e., slow frontocortical and fast centro-parietal spindles.

Design: Two experiments were performed in healthy humans (24.5 ± 0.9 y) investigating undisturbed sleep (Experiment I) and the effects of prior learning (word paired associates) vs. non-learning (Experiment II) on multichannel EEG recordings during sleep.

Measurements and Results: Only fast spindles (12-15 Hz) were synchronized to the depolarizing SO up-state. Slow spindles (9-12 Hz) occurred preferentially at the transition into the SO down-state, i.e., during waning depolarization. Slow spindles also revealed a higher probability to follow rather than precede fast spindles. For sequences of individual SOs, fast spindle activity was largest for "initial" SOs, whereas SO amplitude and slow spindle activity were largest for succeeding SOs. Prior learning enhanced this pattern.

Conclusions: The finding that fast and slow spindles occur at different times of the SO cycle points to disparate generating mechanisms for the 2 kinds of spindles. The reported temporal relationships during SO sequences suggest that fast spindles, driven by the SO up-state feed back to enhance the likelihood of succeeding SOs together with slow spindles. By enforcing such SO-spindle cycles, particularly after prior learning, fast spindles possibly play a key role in sleep-dependent memory processing.

Keywords: Human, memory, sleep spindles, slow oscillations

Citation: Mölle M; Bergmann TO; Marshall L; Born J. Fast and slow spindles during the sleep slow oscillation: disparate coalescence and engagement in memory processing. *SLEEP* 2011;34(10):1411-1421.

INTRODUCTION

Electrical oscillations of brain activity coordinate information transfer and spike time dependent plasticity between different brain circuits and regions.[1] Slow wave sleep (SWS) is characterized by the occurrence of two distinct oscillatory phenomena, i.e., the EEG slow oscillation (SO) and spindle activity, both of which are implicated in memory consolidation and synaptic plasticity during sleep.[2-8] The SO occurs in humans at a peak frequency of ~0.75 Hz and is primarily generated within neocortical networks.[9-15] It synchronizes neuronal activity into generalized down-states (hyperpolarization) of global neuronal silence and subsequent up-states (depolarization) of increased wake-like neuronal firing, not only in the neocortex but also via efferent pathways in other brain regions, including the thalamus as the source of spindle activity. There is compelling evidence that the depolarizing SO up-state via cortico-thalamic volleys drives the generation of spindle activity spreading back in turn from the thalamus to the neocortex.[13,16-18] Accordingly, spindle activity becomes temporally grouped by the SO occurring preferentially during the depolarizing phase of the SO. Likewise, learning-dependent increases in spindle activity are restricted to the SO up-state.[19,20] Spindles occurring in emergent up-states are considered a key mechanism of long-term memory storage in neocortical networks because via massive Ca^{2+} influx into pyramidal cells they are able to promote lasting plastic synaptic changes.[2,21-23]

There is growing evidence for the existence of 2 types of spindles during SWS which differ in frequency and topography, i.e., the "slow" spindles (< 12 Hz) that are dominant over frontal cortical sites and the "fast" spindles (> 12 Hz) that show a more widespread distribution over parietal and central sites.[24-26] Correspondingly, low-resolution brain electromagnetic tomography revealed 2 separate cortical spindle sources, one for slow spindles in a medial frontal region and another for fast spindles in the precuneus.[25] Functional magnetic resonance imaging indicated distinct patterns of brain activation associated with the 2 types of spindles.[27] Beyond common activity in the thalamus and superior temporal gyri, slow spindles were associated with increased activity in the superior frontal gyrus, whereas fast spindles recruited a set of cortical regions involved in sensory motor processing, as well as the medial frontal cortex and hippocampus. A functional differentiation has been suggested, whereby slow frontal spindle activity predominantly reflects a coupling among cortical networks, whereas faster parietal spindle activity is more closely related to thalamo-cortical coupling.[28]

Considering the temporal grouping of spindles by the SO a key mechanism underlying sleep-dependent memory consolidation,[7] we asked whether this effect pertains both to the slow frontal and fast centro-parietal spindles. Specifically, we aimed at characterizing the temporal relationships between SO down- and up-states and the 2 types of sleep spindles during human SWS under basal conditions as well as after learning.

Submitted for publication November, 2010
Submitted in final revised form May, 2011
Accepted for publication June, 2011

Address correspondence to: Matthias Mölle, Department of Neuroendocrinology, University of Lübeck, Ratzeburger Allee 160, Hs. 50, 23538 Lübeck, Germany, Tel: +49 451 500 3643; Fax: +49 451 500 3640; E-mail: moelle@kfg.uni-luebeck.de

METHODS

Subjects and Procedures

Two experiments (I and II) were performed. Eleven healthy men aged 19-33 y (mean 25.8 y) participated in Experiment I. In Experiment II, 10 volunteers participated (5 men, aged 20-29 y, mean 23.1 y). Recordings of Experiment II were taken from a sample of subjects participating in a series of (unpublished) experiments exploring memory functions of sleep. To accustom subjects to sleeping under laboratory conditions, all subjects spent an adaptation night in the sleep laboratory, including the placement of electrodes. The experiments were approved by the ethics committee of the University of Lübeck. Written informed consent was obtained from all subjects prior to participation.

In Experiment I, sessions started at 21:00, with preparing the subject for standard polysomnography and continuous EEG recordings during the subsequent night. Lights were turned off at 23:00, and subjects were awakened at 07:00. In Experiment II (testing the effects of learning on the sleep EEG), subjects slept in the laboratory on 2 experimental nights (between 23:00 and 07:00), i.e., one night (learning condition) that took place after the subjects had performed on a learning task, and another night (non-learning condition) which took place after performance on a non-learning control task. The subject's 2 nights were separated by ≥ 7 days, and the order of conditions was balanced across subjects. In both learning and non-learning conditions, subjects performed the respective tasks between 21:30 and 22:30. The task in the learning condition was a paired words associated learning task, whereas the non-learning task required the subjects to count the occurrence of certain letters in word pairs presented. The tasks have been described in detail previously.[4] Briefly, on the learning task, subjects learned a paired-associate list of 336 unrelated words, arranged in 21 groups of 8 pairs (e.g., factory–horse, circle–scarf). Each group of pairs was presented twice for 106 and 70 sec on the first and second run, respectively, resulting in a total learning time of 61.6 min. To induce comparable mnemonic strategies, subjects were instructed to visually imagine a relation of the 2 otherwise unrelated words of each pair. Recall was tested immediately after the second run of presentation by a cued recall test. The non-learning task was designed to resemble the learning task in as many ways as possible but without the intentional learning component. On this task subjects were instructed to count all letters containing curved lines (e.g., J, P, U, but not W, Y, K) on word-pair stimulus displays identical to those used for the learning task. Thus, visual input, task duration, and difficulty were equal in both conditions, but subjects had little possibility to semantically process the words.

Sleep EEG Recordings, Identification of Slow Oscillations and Spindles

EEG recordings in Experiment I were obtained from 27 channels according to an extended 10-20-System (F3, F1, Fz, F2, F4, FC5, FC3, FC1, FC2, FC4, FC6, C5, C3, C1, Cz, C2, C4, C6, CP5, CP3, CP1, CP2, CP4, CP6, P3, Pz, P4; cap with Ag-AgCl ring electrodes) and both mastoids (A1, A2) referenced to Cz. Before applying caps, subjects' head size was measured and an adequate capsize was chosen. Chest belts (or alternatively chin belts) were used to fixate the caps. Electrode impedances were always kept below 5 kOhm before the start of recordings. EEG signals were offline re-referenced to averaged A1 and A2. Additionally, horizontal and vertical eye movements and the electromyogram from the chin muscles were recorded with Ag-AgCl cup electrodes. The raw EEG signals were amplified (10000-fold), filtered between 0.05 and 100 Hz (plus 50-Hz notch), and digitized at 500 Hz per channel (SynAmps, 16-bit-ADC; Neuroscan, El Paso, TX, USA). Recordings in Experiment II were essentially the same as in Experiment I, except that the EEG was obtained from a restricted sample of 13 electrode sites (F3, Fz, F4, FC3, FC4, C3, Cz, C4, CP3, CP4, P3, Pz, P4).

Sleep stages (1, 2, 3, 4, and REM sleep), awake time, and movement artifacts were scored offline for 30-sec epochs according to standard criteria.[29] Stage 2 sleep corresponds to light NREM sleep, and stages 3 and 4 correspond to slow wave sleep (SWS). After sleep scoring, all EEG data were thoroughly inspected for artifacts, and epochs showing any kind of artifacts (such as noisy signal due to reduced electrode contact, slow EEG drifts because of sweating, increased 50 Hz noise) were marked as epochs to be excluded in the following analyses. EEG data were additionally subjected to a first power analysis by fast Fourier transformations (FFT), performed on subsequent blocks of 4,096 data points (~8 sec of EEG data, 4 blocks per 30-sec epoch). Average power spectra were calculated in all EEG channels, separately for all NREM stage 2 sleep and all SWS epochs of the whole night (Figure S1). In Experiment II, calculation of power spectra and subsequent identification of SOs and spindles concentrated on the first 45 min of SWS, which was done because in most previous studies the effects of learning on sleep EEG parameters were most pronounced for the first sleep cycle (e.g., Gais et al. and Huber et al.).[4,30]

Slow oscillations

Detection of SOs in NREM sleep stage 2 and SWS was based essentially on a standard algorithm described elsewhere in detail.[14] Since slow oscillations showed the typical fronto-central maximum in the power spectrum (Figure S1B) the detection was limited to the 8/6 (Exp. I/Exp. II) fronto-central channels that (during SWS) expressed the largest power in the SO frequency range (i.e. in Exp. I, F3, F1, Fz, F2, F4, FC1, FC2, and Cz; Figure S1B). In a first step, the EEG was low-pass filtered with 30 Hz and down-sampled to 100 Hz. For the identification of large SOs, a low-pass filter of 3.5 Hz was applied to the EEG, and time points of positive to negative zero crossings were computed in the resulting signal. Then, the lowest and highest value between every 2 of these time points were detected (i.e., one negative and one positive peak between 2 succeeding positive to negative zero crossings). Intervals of positive to negative zero crossings with a length of 0.9 to 2 sec were marked as SO epochs if the corresponding negative peak amplitude was lower than −80 μV and the corresponding amplitude difference (positive peak minus negative peak) was ≥ 140 μV. Averages of original EEG potentials in a 2.6-sec window ± 1.3 sec around the peak of the negative half-wave of all detected SOs were calculated.

Spindles

Slow spindles were identified during NREM sleep stage 2 and SWS in those 12 fronto-central channels that expressed the largest power in the slow spindle frequency range (9-12 Hz;

Figure S1B). These were (in Exp. I): F3, F1, Fz, F2, F4, FC3, FC1, FC2, FC4, C1, Cz, C2. Fast spindles were identified during NREM sleep stage 2, and SWS in those 12 centro-parietal channels that expressed the largest power in the fast spindle frequency range (12-15 Hz; Figure S1B). These were (in Exp. I): C3, C1, Cz, C2, C4, CP3, CP1, CP2, CP4, P3, Pz, P4 (Figure S1B). For each subject, peak frequency of slow and fast spindle activity was identified in the channels of interest in the spectra. Subsequently, the EEG was first filtered with a band-pass of ± 1.5 Hz around this peak frequency of slow and fast spindle activity, respectively. For fast spindle activity, a clear peak in the power spectra was detectable in all subjects. In subjects where no discrete slow spindle peak was detectable (2 for SWS and 4 for stage 2 sleep), a band-pass of ± 1.5 Hz around the mean slow spindle peak frequency across the remaining subjects was used. After filtering, a thresholding algorithm was applied that had proven effective in previous studies[4,14] and was the same for detecting slow and fast spindles, respectively. First the root mean square (RMS) of the filtered signal was calculated at every sample point using a moving window of 0.2 sec. The resulting RMS signal was smoothed with a moving average of 0.2 sec. The threshold for spindle detection in the RMS signal was set to 1.5 standard deviations of the filtered signal, as defined by the mean across the 12/8 (Exp. I/Exp. II) fronto-central channels and 12/8 (Exp. I/Exp. II) centro-parietal channels, respectively, and in Experiment II, additionally across the learning and non-learning conditions. A spindle was detected when the RMS signal remained above the threshold for 0.5-3 sec and the beginning and end of the spindle were marked at the threshold crossing points. For every detected spindle, the peaks and troughs were detected as the maxima and minima of the filtered signal (between the beginning and end of the spindle) and the deepest trough was designated as the "spindle peak" that represented the respective spindle in time, i.e., the time point taken for referencing event correlation histograms (see below).

Analyses of Temporal Relationships between Fast and Slow Spindles and SOs

To investigate the temporal relationships between slow spindles, fast spindles, and SOs, 4 types of event correlation histograms of spindle activity were calculated using 6-sec windows with 3-sec offsets and a bin size of 50 msec. The histograms were referenced to the spindle peaks or negative half-wave peaks of the SO, respectively. For "spindle activity," all detected spindle peaks and troughs of all detected spindles were taken (from all channels). The counts in every bin were divided by the number of spindles or SOs used as reference, and then divided by the bin width to give event rate per second (Hz). The first event correlation histogram calculated slow spindle activity referenced to the peak of fast spindles. Conversely, the second histogram calculated fast spindle activity around the peak of slow spindles. The third and fourth event correlation histograms calculated fast and slow spindle activity with reference to the negative half-wave peak of SOs. In order to test whether the event correlation histograms indicated reliable time relationships a randomization procedure was applied on the data in which we randomized the time points of all detected spindles and slow oscillations, used as reference points (0 sec) in the event correlation histograms (i.e., the largest troughs for the spindles and the negative half-wave peaks for the SOs). Then we recalculated the event correlation histograms using as spindle events all originally detected spindle peaks and troughs. Randomization of time points was done by adding a random time between −10 and 10 sec to each time point. Randomization was performed separately for each subject. After recalculation of individual event correlation histograms, means across all subjects were calculated. In order to visualize how slow and fast spindle activity are organized by the SOs, we additionally calculated time-frequency plots of power in all EEG channels in a time window ± 2 sec around the negative peak of SOs. Sequences of SOs in Experiment II were basically analyzed in the same way as single SOs. To focus on the sequential features in SO-spindle interactions, this analysis was restricted to trains of at least 3 succeeding SOs.

Statistical analyses generally relied on paired *t*-tests and analyses of variance (ANOVA), unless specified otherwise. For paired *t*-tests a Bonferroni corrected level of significance for multiple testing was applied, and only significances reaching this level are reported. Paired *t*-tests were performed for the following comparisons: the number of detected slow oscillations during SWS and S2 sleep, mean peak frequency for slow spindles during SWS and S2 sleep, and average potential levels during the 300-msec intervals preceding and following the peaks of slow and fast spindles.

Effects on event-correlation histograms were first evaluated using ANOVA including a repeated measures factor "Time," reflecting the different time points with reference to 0 sec. Analyses of spindle data included an additional "Type" of spindle factor (fast vs. slow), and analyses of SO sequences an additional factor "Position" (initial, middle, final). Data from Experiment II included an additional "Learning" factor. Only if the main and interaction effects of interest regarding the Time, Type, Position, or Learning factor revealed to be significant, further post hoc pairwise testing was performed (and reported here).

Reported correlations (density of slow spindles with the density of SOs and peak negativity of the prefrontal SO and the RMS amplitude of concurrent slow frontal spindle activity) were tested at an explorative level and not corrected for multiple testing.

RESULTS

Temporal Relationship between Fast and Slow Spindles and Slow Oscillations: Experiment I

Polysomnographic sleep parameters confirmed that our subjects' sleep was within the normal range (Table 1). The proportion of SWS was 16.6% ± 1.3% and of stage 2 sleep 55.7% ± 2.1%. As expected, power within the SO frequency band (~0.5-1.3 Hz) was distinctly higher during SWS than stage 2 sleep, and the number of detected SOs was also distinctly greater in SWS ($P < 0.001$, Table 2). Power spectra of both, stage 2 sleep and SWS showed a clear peak for fast spindle activity, with a maximum over centro-parietal cortex regions (Figure S1A). In contrast, for slow spindle activity a clear peak was only visible in the grand mean power spectrum of SWS, with a distinct maximum over the frontal cortex. This pattern was likewise apparent in the individual spectra of the 11 subjects. (Note that the clear frontocortical maximum of slow spindles makes them dis-

tinct from alpha activity observed during waking with a maximum over posterior cortical regions, although both oscillatory phenomena overlap in frequency). The mean peak frequency (across subjects) was comparable between SWS (13.40 ± 0.11 Hz) and stage 2 sleep (13.46 ± 0.11 Hz) for fast spindles, but differed for slow spindles (10.23 ± 0.15 in SWS vs. 11.44 ± 0.12 Hz in stage 2 sleep, $P < 0.01$; Figure S1A, and Table 3). Density (per 30-sec interval) was generally lower for slow than fast spindles ($P < 0.001$; Table 2). Because of the distinctly greater number of SOs in SWS than in stage 2 sleep and the weak expression (in terms of power) of slow spindles in the latter stage, we focused on the temporal relationships between SOs and spindles during all SWS epochs of the whole night. Spindles are not always associated to SO. Therefore, as an estimate of the proportion of total spindles during SWS that indeed occurred in temporal association with SO, we determined the number of spindles of all spindles identified during SWS which occurred in an interval of ± 3 sec around the negative peak of a detected SO. The analysis revealed a proportion of 60.4% ± 5.0% of all fast spindles and of 70.3% ± 4.8% of all slow spindles that during SWS occurred within ± 3 sec around the negative peak of a detected SO.

In order to examine the general structure of the detected spindles independently of the slow oscillations, we averaged the original EEG signal time-locked to all fast and slow spindles detected during SWS (using the deepest, i.e., most negative trough in the filtered signal as reference; Figure 1). The comparison of average potential levels during the 300-msec intervals preceding and following the spindle peak indicated strong and systematic slow potential shifts underlying the 2 types of spindles: Whereas this background potential level during fast spindles increased from −4.19 ± 1.87 μV (before spindle peak) to +3.63 ± 1.52 μV (after spindle peak, $P < 0.001$), it strongly decreased from +1.77 ± 1.93 to −11.78 ± 2.08 μV ($P < 0.001$) for slow spindles. In fact, as shown in Figure 1, whereas fast spindles appear to ride on the positive going upward potential shift of the SO, the course of slow frontal spindles largely coincides with the negative going downward potential shift of the SO. Interestingly, topographical analyses revealed that the positive potential shifts underlying fast spindles were larger the more posterior the fast spindles occurred. Conversely, the negative potential shifts in the slow spindles became larger the more anterior the slow spindles occurred (Figure S2).

Event correlation histograms indicated a clear temporal relationship between the 2 types of spindles (Figure 2). Fast spindles were followed by an increase in slow spindle activity with a delay of ~500 ms ($P < 0.001$, for comparing the 0.25…0.75-sec epoch with the −3.0…−2.5-sec epoch used as baseline reference; Figure 2A). Slow spindles, conversely, were preceded (by ~500 ms) by a distinct increase in fast spindle activity ($P < 0.001$, for −0.75…−0.25-sec epoch vs. baseline; Figure 2B). In combination, these temporal relationships are consistent with a causal impact of fast centro-parietal spindles on

Table 1—Polysomnographic sleep parameters

Parameter	Exp. I	Exp. II Learning	Exp. II Non-Learning
TST	432.3 ± 9.7 min	430.7 ± 15.4 min	450.0 ± 20.1 min
Wake	2.8 ± 1.2 min	11.2 ± 2.4 min	7.1 ± 1.9 min
S1	1.5 ± 0.2%	11.2 ± 1.9%	9.8 ± 2.0%
S2	55.7 ± 2.1%	59.7 ± 1.9%	58.8 ± 1.3%
SWS	16.6 ± 1.3%	11.7 ± 1.3%	12.9 ± 1.3%
REM	26.2 ± 1.9%	17.4 ± 1.6%	18.6 ± 1.7%
SOL	3.9 ± 0.9 min	8.7 ± 1.5 min	6.9 ± 1.3 min

TST, total sleep time; S1 and S2, NREM sleep stages 1 and 2; SWS, slow wave sleep; SOL, sleep onset latency. Percentages are given with reference to TST. Means (± SEM) are reported.

Table 2—Mean sleep spindle density (averaged across 12 channels) and slow oscillation density (across 8 channels) during SWS and stage 2 sleep in (number per 30 sec)

	SWS			Stage 2		
Subject	Slow Spindles	Fast Spindles	SO	Slow Spindles	Fast Spindles	SO
1	1.16 (156.5)	2.23 (301.6)	2.74 (369.3)	1.69 (704.8)	2.29 (955.3)	0.61 (256.8)
2	1.25 (181.3)	2.78 (403.3)	3.80 (550.8)	2.36 (869.2)	2.86 (1054.2)	0.40 (148.3)
3	1.57 (193.4)	2.79 (342.6)	3.51 (431.1)	2.71 (1268.8)	3.22 (1506.3)	1.27 (593.6)
4	2.49 (461.4)	2.85 (526.9)	3.52 (652.0)	2.43 (1198.6)	3.04 (1501.3)	1.30 (639.9)
5	2.12 (171.6)	2.82 (228.6)	0.83 (67.6)	2.18 (1109.6)	2.81 (1428.5)	0.43 (216.7)
6	1.15 (131.8)	3.10 (356.3)	1.06 (122.4)	2.19 (942.9)	3.49 (1504.3)	0.21 (92.4)
7	2.41 (342.0)	2.67 (379.3)	2.62 (372.1)	2.02 (751.7)	3.17 (1182.1)	0.46 (172.3)
8	1.00 (96.7)	1.78 (172.8)	1.64 (158.8)	1.75 (742.3)	2.93 (1243.9)	0.39 (165.2)
9	1.48 (148.3)	2.34 (233.7)	4.13 (412.5)	2.01 (1081.0)	2.62 (1408.2)	0.86 (464.6)
10	2.11 (333.2)	2.20 (347.5)	1.94 (306.1)	2.11 (884.7)	2.66 (1112.5)	0.82 (344.8)
11	2.01 (400.8)	2.28 (454.3)	3.97 (791.0)	2.37 (1006.4)	2.74 (1160.1)	0.82 (346.2)
Mean ± SEM	1.70 ± 0.16 (237.9 ± 37.2)	2.53 ± 0.12 (340.6 ± 31.2)	2.71 ± 0.36 (384.9 ± 67.0)	2.16 ± 0.09 (960.0 ± 57.3)	2.89 ± 0.10 (1277.9 ± 60.2)	0.69 ± 0.11 (312.8 ± 55.6)

Values in parentheses show mean number of detected spindles and slow oscillations averaged across the same channels.

slow frontal spindles, but do not support the opposite relationship.

Additionally, event correlation histograms indicated a consistent timing of the 2 kinds of spindles during the SO cycle. As expected[14]—with reference to the negative half-wave peak of the SO—fast spindle activity was strongly suppressed around the SO down-state ($P < 0.001$, for −0.3…0.2 sec compared to baseline) and showed a pronounced increase during the transition to the up-state ($P < 0.001$, for 0.4…0.9 sec compared to baseline; Figure 2C). Interestingly, this strong increase in fast spindle activity during the SO up-state was followed by a prolonged (2-3 sec) period of slightly suppressed fast spindle activity ($P < 0.01$). Fast spindle activity was also enhanced between ~1000-500 ms before the negative SO half-wave ($P < 0.001$), although to a lesser degree than during the SO up-state (following the SO down-state), which likely reflects up-state related activity of the preceding SO. Like fast spindle activity, slow spindle activity also showed 2 distinct maxima with reference to the negative half-wave peak of the SO, which occurred, however, at times different from those of fast spindle activity. The first (and larger) maximum was reached immediately (~150 ms) before the negative SO peak ($P < 0.01$, for −0.4…0.1 sec compared to baseline; Figure 2D), which means that slow spindle activity is highest exactly during the transition into the SO down-state. The second maximum of slow spindle activity peaked ~1000 ms following the negative half-wave peak, i.e., ~500 ms following the pronounced increase in fast spindle activity associated with the SO up-state ($P < 0.01$, for 0.75…1.25 sec compared to baseline). The reliability of these temporal relationships was further confirmed by event correlation histograms constructed from randomized data. Indeed, none of the significant effects observed in the event correlation histograms of the original data survived after randomization of the time points ($P > 0.3$, uncorrected). Moreover, it was confirmed that the intervals in the event correlation histograms of the original (i.e., non-randomized) data, which significantly differed from baseline, were also significantly different from the corresponding intervals for the randomized data.

The temporal relationships between spindles and SOs were further specified in time-frequency plots of spindle wavelet-power (± 1.2 sec around the negative SO peak; Figure 3A, Figure S3), indicating for fast spindle activity (> 12 Hz) the expected suppression during the SO down-state (around 0 sec) and distinct enhancements during both the preceding and following SO up-state. For slow spindle activity (< 12 Hz), the plots confirm a strong transient enhancement during the transition into the SO down-state and a clear suppression during the transition into the following SO up-state (Figure 3B). Although observable at all 27 recording sites, the modulation of fast spindle activity was strongest in the middle centro-parietal channels and of slow spindle activity in the frontal channels, i.e., the respective sites of maximum spindle power (Figures S3, S4).

We further explored the unexpected association of slow spindles with the transition into the negative SO down-state, ap-

Table 3—Spindle peak frequencies (Hz)

	SWS		Stage 2	
Subject	**Slow Spindles**	**Fast Spindles**	**Slow Spindles**	**Fast Spindles**
1	10.96	13.94	11.54	13.85
2	*	13.10	*	13.00
3	10.02	13.17	11.64	13.37
4	9.79	13.71	11.66	13.65
5	10.60	13.67	11.11	13.97
6	*	13.42	*	13.24
7	10.17	13.95	11.05	14.03
8	9.44	13.13	*	13.28
9	10.44	13.38	11.19	13.49
10	10.56	12.86	*	12.99
11	10.07	13.12	11.90	13.20
Mean ± SEM	10.23 ± 0.15	13.40 ± 0.11	11.44 ± 0.12	13.46 ± 0.11

*No peak detectable in the power spectra

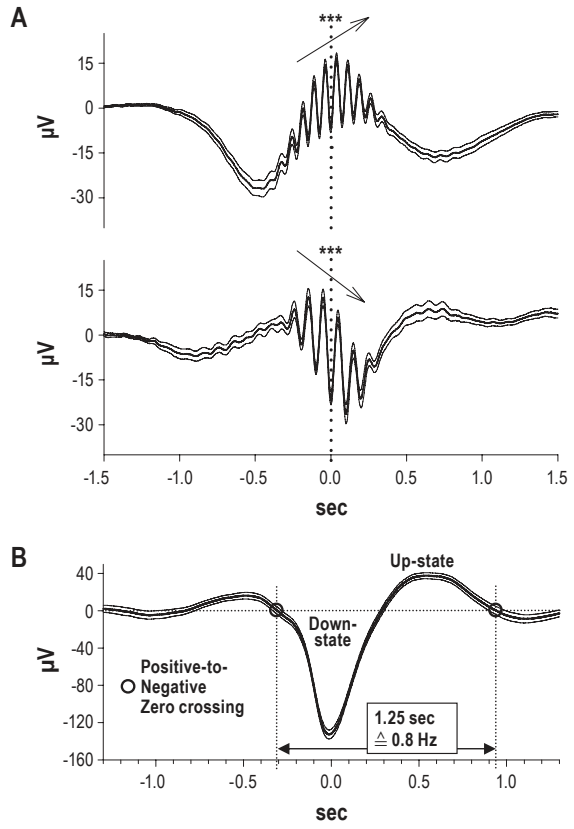

Figure 1—Averaged fast and slow spindles and averaged slow oscillations. **(A)** Grand mean averages (± SEM) of original EEG in (top) 12 centro-parietal channels across all detected fast spindles and (bottom) in 12 fronto-central channels across all detected slow spindles. Note, spindles are averaged independently of whether an SO was present. Averaging was performed with reference to the deepest, i.e., most negative, trough in the filtered signal (t = 0). Asterisks (and arrows) indicate a significant ($P < 0.001$) positive and negative slow potential shift underlying fast and slow spindles, respectively, in the interval between 300 ms before to 300 ms after the spindle peak. **(B)** Grand mean averages (± SEM) of original EEG in 8 fronto-central channels across all detected slow oscillations. Averaging was performed with reference to the negative half-wave peak of the SO (t = 0). Indicated is also the time interval between 2 succeeding positive-to-negative zero crossings of the EEG signal which was used to identify SOs (see Methods).

plying correlation analyses (on mean spindle and SO measures in the 5 frontal EEG channels of interest). The density of slow spindles, i.e., their rate per 30-sec SWS, was only moderately correlated with the density of SOs in the prefrontal channels ($r = 0.27$, $P < 0.05$), reflecting that slow spindles only irregularly occurred during a SO. In order to examine whether slow spindles if coinciding with a SO could basically enhance the negative amplitude of this oscillation, we calculated correla-

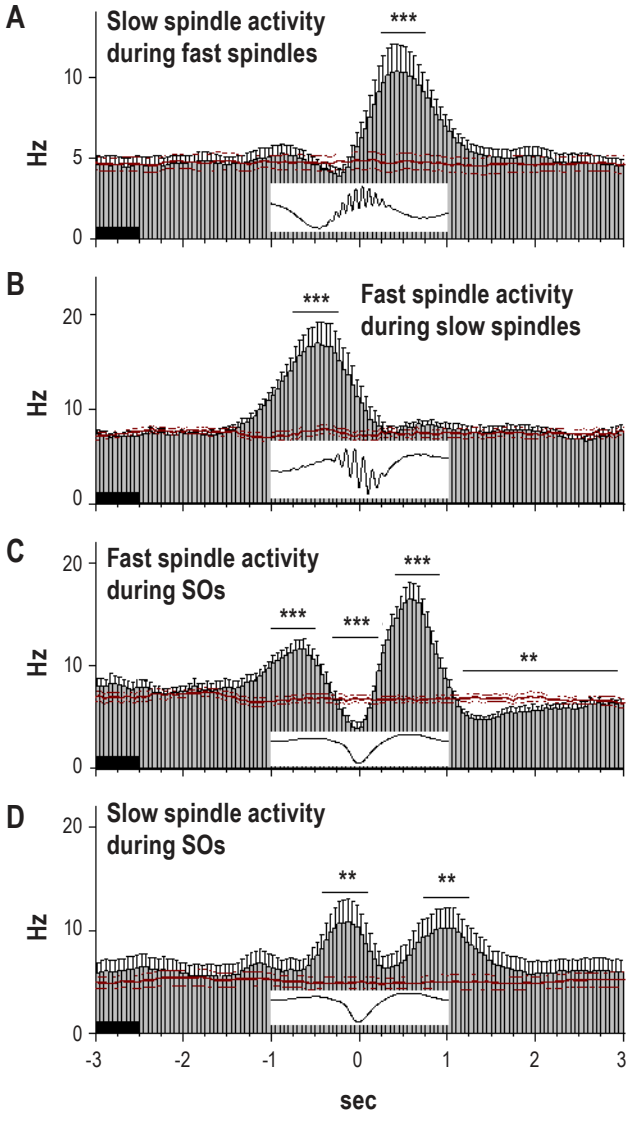

Figure 2—Temporal association between fast and slow spindles and SOs. Event correlation histogram **(A)** of slow spindle activity (i.e., all marked peaks and troughs of all detected spindles) with reference to the peak (most negative trough; t = 0) of fast spindles; **(B)** of fast spindle activity with reference to the peak of slow spindles; **(C)** of fast spindle activity with reference to the negative peak (t = 0) of the SOs; and **(D)** of slow spindle activity with reference to the negative peak of the SOs. Insets show the respective reference spindle and SO. Red lines indicate mean (± SEM) event correlation histograms obtained after randomization of data. Note in **(A)** and **(B)**, fast spindles are followed (with a 500 ms delay) by an increase in slow spindle activity and, conversely, slow spindles are preceded by an increase in fast spindle activity (500 ms before). Note also in **(C)**, strong increases in fast spindle activity before and after the negative SO down-state coincide with SO up-states and in **(D)**, strong increases in slow spindle activity coincide with the beginning of the downward going negative phase of the SO. Asterisks indicate significant increases and decreases, respectively in spindle activity in the indicated intervals (thin lines) as compared to the 0.5-sec baseline interval (thick line; ***P < 0.001, **P < 0.01).

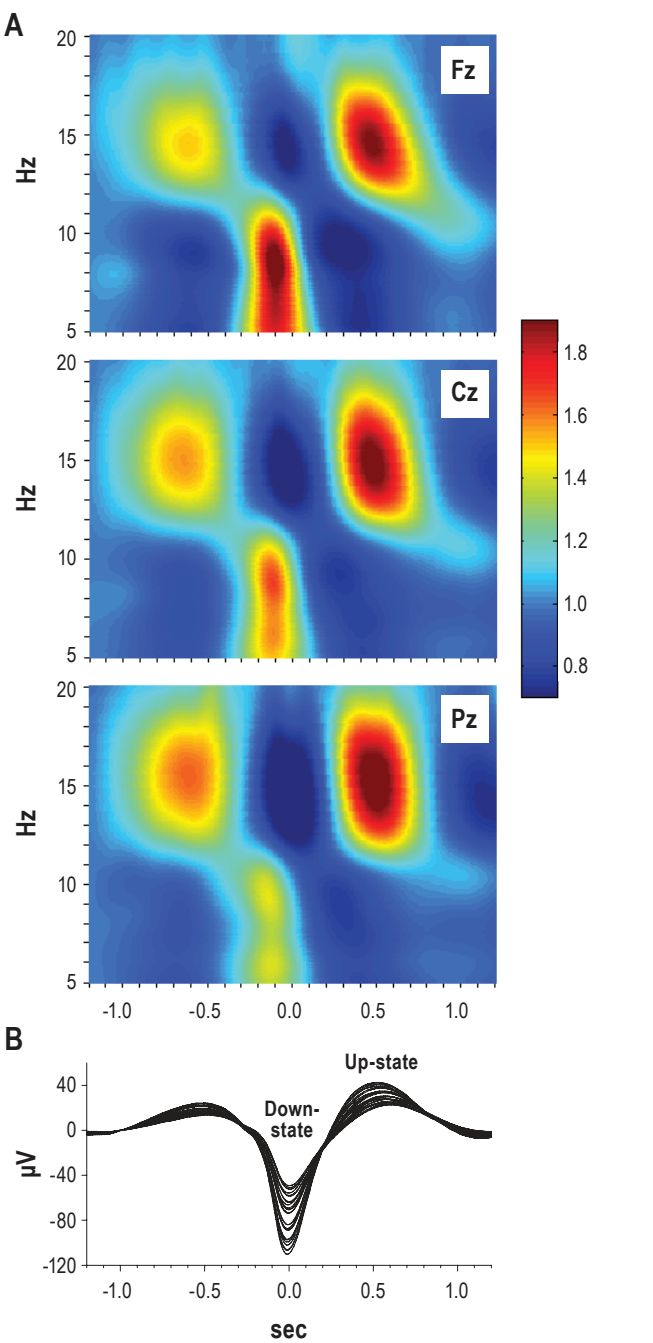

Figure 3—Time-frequency plots of wavelet-power during slow oscillations. **(A)** Time-frequency plots of wavelet-power in a time window of ± 1.2 sec and for frequencies of 5-20 Hz around the negative peak of the SO (t = 0) in the frontal (top), central (middle), and parietal (bottom) electrode. Note, strong enhancement in < 12 Hz slow spindle wavelet-power during the transition into SO down-state most pronounced in the frontal electrode. Coloring indicates relative wavelet-power with the average power during the baseline (−1.3 to −1.2 sec) set to "1." **(B)** Grand mean averages of original EEG in all 27 recording channels across all detected SOs. Averaging was performed in a time window of ± 1.2 sec with reference to the negative peak of SOs (t = 0).

tions between the peak negativity of the prefrontal SO and the (root mean square) amplitude of concurrent slow frontal spindle activity. This correlation revealed to be significant ($P < 0.05$) in all but one subject, but on average again was rather low ($r = 0.14 \pm 0.04$).

Analysis of SO Sequences

Who influences whom in the slow oscillation cycle? To further examine to what extent the 2 spindle types contribute to the emergence of the SO, we analyzed the relationship between spindle activity and SOs in sequences of SOs separately for 4 types of SOs: (i) SOs that were followed but not preceded by another SO ("initial" SOs); (ii) SOs that were preceded and followed by another SO ("middle" SOs); (iii) SOs that were preceded but not followed by another SO ("final" SOs); and (iv) singular SOs that were neither preceded nor followed by another SO ("single" SOs). Calculation of the mean auto-event correlation histogram of all detected SOs assured that SOs tend to occur in groups by indicating a clearly increased probability for a SO to be preceded and/or followed by another SO at about ± 1.25 sec (Figure S5A). Peak-to-peak amplitudes of middle SOs were significantly higher than for all other types of SOs (refer to Figure 4 for statistical comparisons, Figure S5B). Interestingly, contrasting with the distribution of SO peak-to-peak amplitude the increase in fast spindle wavelet-power during the SO up-state was most pronounced not for the highest SOs (i.e., the middle SOs), but for initial SOs, i.e., the first SOs in sequences of SOs. The strong increase in fast spindle power during these initial SOs suggests a particular importance of this type of spindles for initiating further SOs and associated slow spindle events. On the other hand, the increase in slow spindle wavelet-power during transitions into the SO down-state varied in parallel with the SO peak-to-peak amplitude, with these variations overall only approaching clear statistical significance (Figure 4).

Effects of Prior Learning: Experiment II

In a separate study (Experiment II), we examined how learning of a hippocampus-dependent task (paired-associate words) affects the relationship between fast and slow spindles and SOs. We focused this analysis on sequences of SOs. (Refer to Table 1 for polysomnographic data). Although the number of SOs (identified during the first 45 min of SWS) did not differ between the learning (326.1 ± 28.7) and non-learning (345.4 ± 28.7) condition ($P > 0.6$), for all subsequent analyses we normalized data with reference to the respective SO numbers. Mean auto-event correlation histograms of SOs for the learning and non-learning condition, besides confirming the general tendency of SOs to occur in trains, indicated that after learning the occurrence of trains of several succeeding SOs was distinctly enhanced ($P < 0.001$ for the intervals between −1.8…−1.0 sec before and 1.0…1.8 sec after an SO, Figure 5A). Event correlation histograms of fast and slow spindle events calculated with reference to the negative peak of the SOs confirmed the consistent timing of these spindles during the SO cycle (Figure 2C, D); i.e., fast spindles occurred preferentially during the depolarizing SO up-state, whereas slow spindles occurred preferentially during the transition into the down-state (Figure 5B, C). Importantly, these histograms revealed that compared with the non-learning condition, after learning the SOs were preceded by distinctly enhanced fast spindle activity ($P < 0.001$, for −2.5…−0.8 sec before the negative SO peak, Figure 5B), and followed by en-

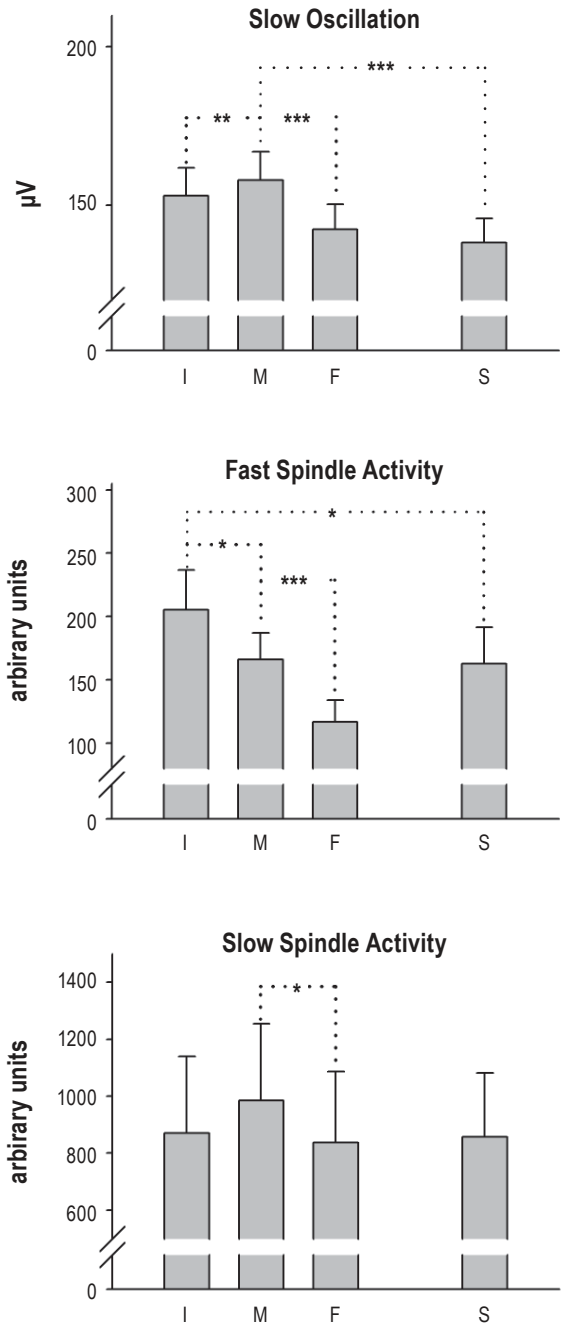

Figure 4—Analyses of sequences of slow oscillations. Upper panel: Mean (+ SEM) peak-to-peak SO amplitudes (in the −0.2 to 0.7 sec interval) for the 4 types of SOs (across 8 fronto-central channels). Middle and lower panels: Mean (+ SEM) amplitude (peak-to-peak wavelet-power in the −0.3 to 0.8 sec interval) of increase in fast spindle wavelet power (during SO up-state) and slow spindle wavelet power (during transition into SO down-state) for 4 types of SOs (averaged, respectively, across 12 centro-parietal and 12 fronto-central recording sites of interest; n = 11). I, M, F: initial, middle, final SO in a SO sequence, S: single SO. Asterisks indicate significant differences in peak-to-peak SO amplitude and spindle wavelet-power, respectively between the different types of SOs (***$P < 0.001$, **$P < 0.01$, *$P < 0.05$).

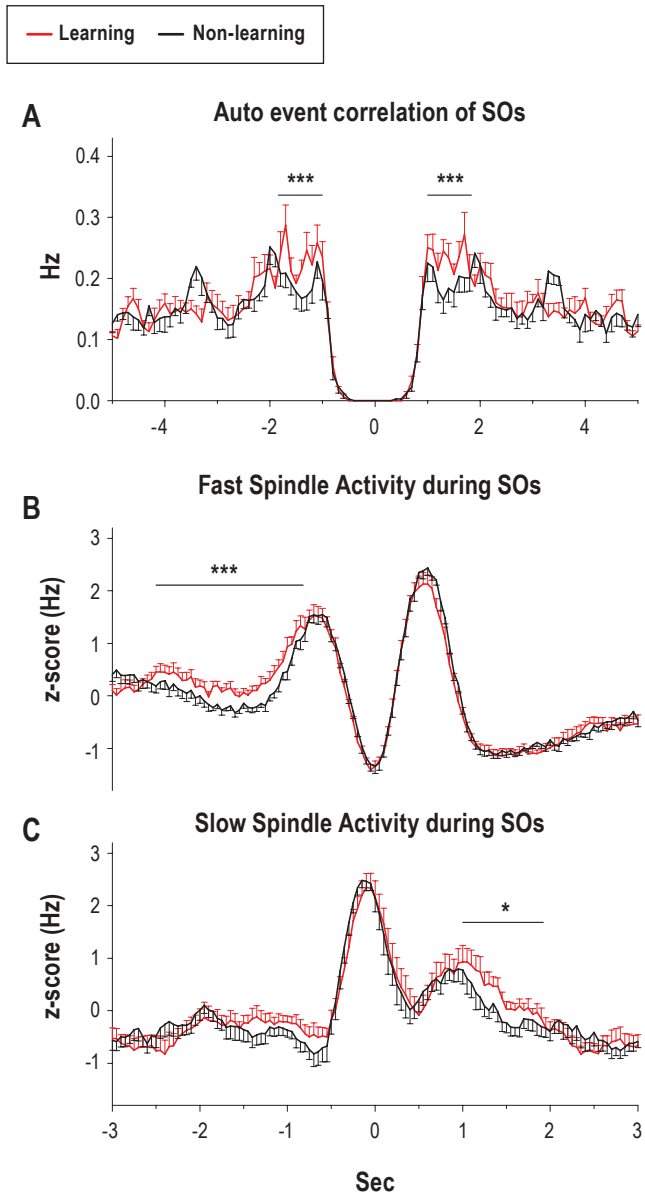

Figure 5—Effects of learning on slow oscillations and associated fast and slow spindle activity. **(A)** Auto-event correlation histogram of all detected SOs after Learning (red) and Non-learning (black). SOs were identified in an average channel across the 6 fronto-central channels of interest. **(B)** Event correlation histogram of fast spindle activity and **(C)** of slow spindle activity, both with reference to the negative peak of the SOs, after Learning (red) and Non-learning (black). Spindle activity was defined by all peaks and troughs of all detected spindles (averaged across the 8 channels of interest), and z-transformed for each subject. For all 3 histogram panels, means (± SEMs) are shown. ***P < 0.001, *P < 0.05, for pairwise comparisons between Learning and Non-Learning).

hanced slow spindle activity (P < 0.05, for 1.0…1.9 sec after the SO; Figure 5C).

How does learning before sleep influence trains of SOs and the distribution of associated slow and fast spindle activity? Averages of the original EEG (during epochs of identified SOs) revealed most consistent effects of learning for middle SOs. In these SOs, up-state depolarization shortly before the transition into the down-state was larger after learning than non-learning (P < 0.01, for −0.5…−0.25 sec before the negative peak of the SO; Figure 6A). Learning additionally induced a slight increase in positivity following the negative peak of middle SOs (P < 0.05, for +0.47…+0.51 sec). The learning-induced increases in up-state positivity (both before and after the SO down-state) coincided with a markedly enhanced fast spindle activity (for spindle RMS in Cz P < 0.01, for −0.65…−0.35 sec before SO negative peak, and P < 0.01, for 0.5…0.75 sec after the SO negative peak). The learning-dependent enhancement of fast spindle activity was most pronounced when averaged with reference to the negative peak of initial SOs, where it concentrated 0.7…1.1 sec after the negative peak of these SOs (in Cz P < 0.001, Figure 6B) and was smallest for the final SOs. Overall, this pattern suggests a role for learning-induced fast spindle activity in initializing and upholding trains of SOs. In contrast to fast spindle activity, learning-dependent increases in slow spindle activity were less consistent and reached only marginal significance towards the end of a SO train, i.e., in the −0.9…−0.6 sec interval preceding the final SO (P < 0.05; Figure 6C).

DISCUSSION

We provide novel evidence for the existence of two different types of spindles during human SWS which differ in frequency and topography, exhibit a unique temporal relationship to each other and to the SO, and show different sensitivity to prior learning. The three main findings of our study are: (i) only fast spindles, with a spectral peak at 13.4 Hz and a centro-parietal maximum, show the expected synchronization to the depolarizing SO up-state together with a strong suppression during the SO down-state. In contrast, slow frontal spindles, with a spectral peak at 10.2 Hz and a more focused frontal cortical maximum, are obviously associated with the transition into the SO down-state and occur with high probability shortly (~125 ms) before the negative SO peak. Moreover, we found that fast spindles precede slow spindles by about 500 ms. (ii) Analysis of sequences of SOs indicated that power of fast spindles is largest for initial SOs that are followed but not preceded by another SO, whereas SO amplitude itself was largest for middle SOs that were preceded and followed by another SO. (iii) Prior learning increased the occurrence of trains of SOs and fast spindle activity, particularly during initial SOs. In contrast, learning-induced increases of slow spindle activity emerged only towards the end of SO trains.

These findings show that the widely held concept of the emergent depolarizing SO up-state driving thalamic spindle generation accounts only for fast centro-parietal spindles, but not for slow frontal spindles occurring during waning depolarization at the transition into cortical hyperpolarization.[13,16,17,31] The fast centro-parietal spindles themselves appear to play a regulatory role in the slow oscillation cycle by increasing the likelihood of subsequent SOs together with the occurrence of slow frontal spindles during succeeding SOs. By promoting the occurrence of SO trains and associated slow frontal spindle activity, fast spindles may particularly support the processing of newly acquired memories during sleep.

Previous studies have suggested functional differences in fast centro-parietal and slow frontal spindles as revealed by their differential sensitivity to factors such as the duration of prior waking, pharmacological agents, age, and intelligence.[24] The present data corroborate the concept of a distinct class of slow

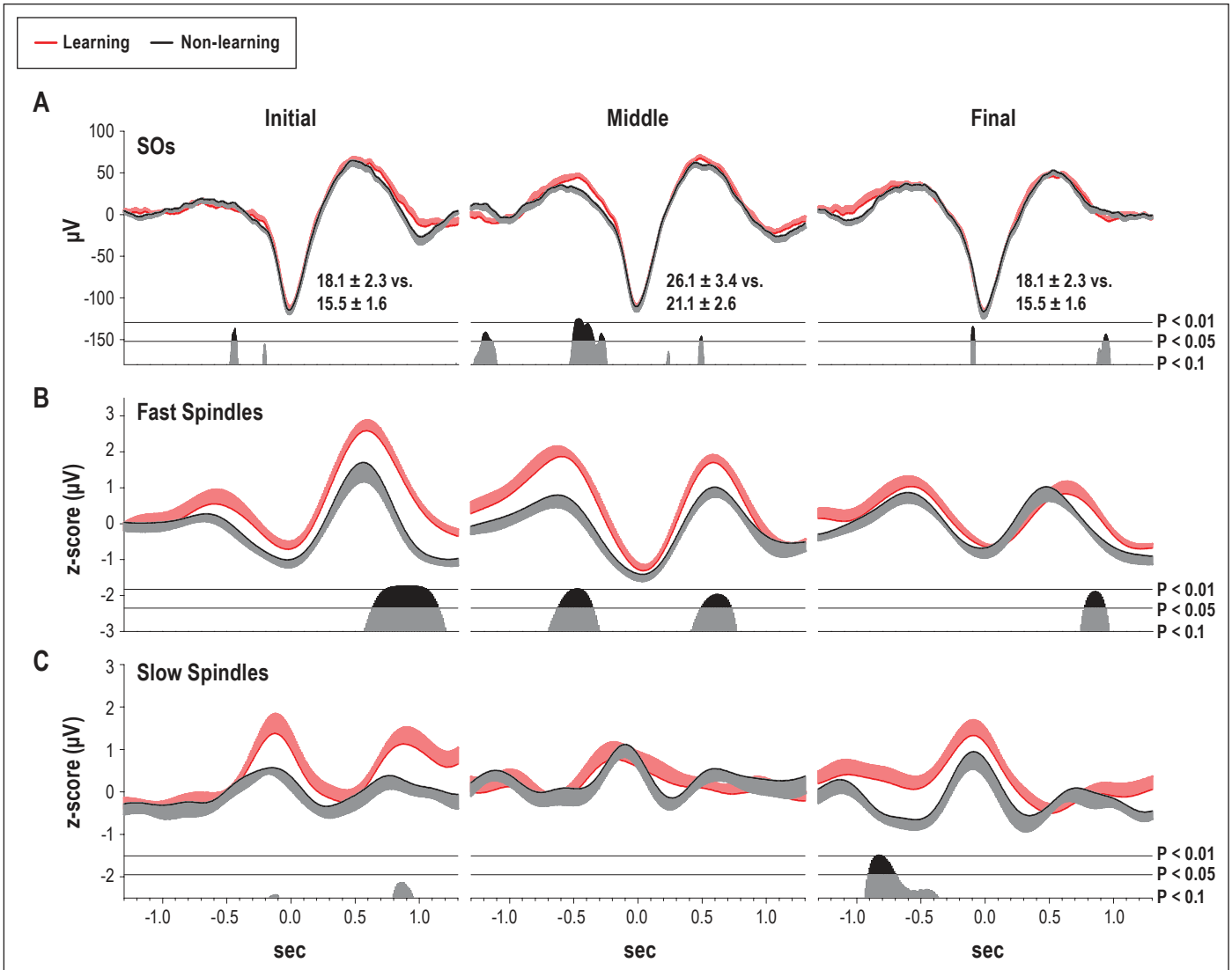

Figure 6—Effects of learning on sequences of slow oscillations. Averages of **(A)** original EEG and RMS activity for **(B)** fast and **(C)** slow spindle frequency range during identified SOs that occurred in sequences for the learning (red) and non-learning (black) condition. Averaging (across identified SO sequences and subjects) for SOs was performed on the original unfiltered signal in the 6 fronto-central channels of interest. Fast and slow spindle RMS activity was averaged, respectively, for the 8 centro-parietal and 8 fronto-central channels of interest. "Initial," "Middle," and "Final" indicate position of target SO in a sequence of (3-5) succeeding SOs. Means (± SEMs) are shown. Bottom bars indicate P-values of paired *t*-tests between Learning and Non-learning condition.

frontal spindles by revealing their differential involvement in the temporal evolution of the SO, thus pointing towards separate generating mechanisms. Studies of the generating mechanisms of spindles were performed mainly in cats and rats without distinguishing prefrontal spindles.[13] Those studies revealed a consistent association of spindles with the emergent SO up-state, reflecting the driving influence of depolarization and increased firing of cortico-thalamic projections on the generation of spindle oscillations in thalamo-neocortical feedback loops.[13,16,17] In contrast, surface-negative components of SOs corresponding to intracellular hyperpolarization were associated with silence in these corticofugal projections and suppression of spindle activity. The occurrence of slow frontal spindles during a time when depolarization was already fading precludes the same generating mechanism for these spindles. Although thalamic activity cannot be excluded as a common source for slow and fast spindles,[27] slow spindles could alternatively be considered primarily of cortical origin, developing in the aftermath of a strong network depolarization. This view would correspond to the idea that slow frontal spindles are functionally associated with cortico-cortical interactions, whereas centro-parietal spindles are linked to activity in thalamo-cortical loops.[28]

Interestingly, there was a small but consistent association of slow spindle power with peak negativity of the prefrontal SO. Likewise, in sequences of SOs slow spindle power was maximal when the SO amplitude was also maximal, which was the case for "middle" SOs. This could reflect that slow spindles once occurring during a SO, add to the hyperpolarizing SO down-state. However, previous findings[6] showed the reverse relationship, such that the hyperpolarizing SO potential provides conditions favoring the emergence of a slow spindle. In those studies, transcranial application of slow potential fields oscillating at the SO frequency (0.75 Hz) not only enhanced endogenous SOs but also concomitant slow frontal spindles.

The emergent hyperpolarizing SO down-state has been linked to several intrinsic currents in cortical neurons, i.e., mainly the activation of Ca^{2+}-dependent potassium currents, the inactivation of the persistent Na^+ current, and the activation of a Na^+-dependent K^+ current that together with activity-dependent synaptic depression induce a general disfacilitation of neuronal excitability. Furthermore, extracellular calcium progressively declines towards the up-to-down state transition.[31-35] Slight displacements in the dynamics of these currents may predispose the network to the generation of slow spindles.

Sequences of SOs

The analysis of trains of SOs revealed remarkable insights into the interrelationship between SOs and the two types of spindles, and its particular sensitivity to prior learning. A most distinct pattern was revealed for the fast spindles. Whereas amplitudes of the SO and slow spindles were maximal for "middle" SOs, the fast spindles were indeed maximal for "initial" SOs and minimal during "final" SOs. This pattern suggests that fast spindles apart from being driven by the depolarizing SO up-state, themselves feed back to promote the generation of succeeding SOs, together with slow spindles. Prior learning enhanced this pattern: i.e., not only was the number of SOs occurring in trains enhanced after learning, but learning also markedly increased fast spindle activity preceding a SO. During SO sequences, the most distinct learning-induced increase in fast spindle activity was revealed for the initial SO, whereas only weak increases occurred during SOs completing a train. Although less robust, a basically reversed pattern became apparent for the slow spindles. Overall, these data suggest a loop-like scenario where the fast centro-parietal spindles, possibly by promoting Ca^{2+} influx into cortical pyramidal cells,[21,35] enhance the likelihood and amplitude of succeeding SOs, as well as of a slow frontal spindle developing during the waning depolarization of these subsequent SOs. Emergent depolarization in this SO cycle, conversely, drives the generation of the next fast centro-parietal spindle, although due to refractoriness, this spindle is slightly lower than the initial one.[36] Prior learning appears to enhance the driving role of the fast spindles in the generation of such SO-spindle cycles. Learning can induce quite robust increases in fast spindle activity also during sleep stage 2, which is less dominated by SOs.[4,37,38] In some studies, fast spindle activity was correlated to overnight retention of memories.[39-41] In combination with those findings, the present data corroborate the view of fast spindles as an essential mechanism for the initiation and maintenance of sleep-dependent memory processing. Although this view integrates evidence relating sleep spindles of stage 2 (rather than SWS) with memory consolidation,[4,37,38,42] it would be premature to generalize a similar immediate temporal coupling with SOs as observed here for spindles in SWS to the spindles of stage 2 sleep. In stage 2 sleep, spindles are likely to occur much more often in the absence of SOs, which, nevertheless, would not preclude that these spindles and associated cellular processes exert a stimulatory influence on SO generating mechanisms.

By promoting synaptic long-term potentiation, spindles can support the long-term storage of memory-related information in neocortical networks.[2] However, this view has been linked to the fast centro-parietal spindles occurring during the depolarizing SO up-state as a phase of increased neuronal excitability. It is currently unclear whether slow frontal spindles that occur during waning SO depolarization can support synaptic plastic processes in a similar way. Whatever the role of slow spindles, as fast centro-parietal spindles tend to precede the slow frontal spindles (by ~500 ms) in the SO cycle, it is tempting to speculate that the two kinds of spindles are associated with succeeding steps in sleep-dependent memory processing: Whereas the fast spindles coinciding with hippocampal sharp wave ripples may represent a mechanism that facilitates the transfer of memory-related information from the hippocampus to the neocortex,[23,43,44] subsequent slow spindles may be related to a cortico-cortical cross-linking of transferred information with prefrontal circuitry. The latter indeed is considered of particular importance in the formation of neocortical long-term memory representations.[28,45-47]

ACKNOWLEDGMENTS

This work was supported by the Deutsche Forschungsgemeinschaft (Project A6, SFB 654 'Plasticity and Sleep').

DISCLOSURE STATEMENT

This was not an industry supported study. The authors have indicated no financial conflicts of interest.

REFERENCES

1. Buzsáki G, Draguhn A. Neuronal oscillations in cortical networks. Science 2004;304:1926-9.
2. Rosanova M, Ulrich D. Pattern-specific associative long-term potentiation induced by a sleep spindle-related spike train. J Neurosci 2005;25:9398-405.
3. Czarnecki A, Birtoli B, Ulrich D. Cellular mechanisms of burst firing-mediated long-term depression in rat neocortical pyramidal cells. J Physiol 2007;578:471-9.
4. Gais S, Mölle M, Helms K, Born J. Learning-dependent increases in sleep spindle density. J Neurosci 2002;22:6830-4.
5. Eschenko O, Mölle M, Born J, Sara SJ. Elevated sleep spindle density after learning or after retrieval in rats. J Neurosci 2006;26:12914-20.
6. Marshall L, Helgadottir H, Mölle M, Born J. Boosting slow oscillations during sleep potentiates memory. Nature 2006;444:610-3.
7. Diekelmann S, Born J. The memory function of sleep. Nat Rev Neurosci 2010;11:114-26.
8. Tononi G, Cirelli C. Sleep function and synaptic homeostasis. Sleep Med Rev 2006;10:49-62.
9. Steriade M, Nunez A, Amzica F. Intracellular analysis of relations between the slow (< 1 Hz) neocortical oscillation and other sleep rhythms of the electroencephalogram. J Neurosci 1993;13:3266-83.
10. Steriade M, Nunez A, Amzica F. A novel slow (< 1 Hz) oscillation of neocortical neurons in vivo: depolarizing and hyperpolarizing components. J Neurosci 1993;13:3252-65.
11. Achermann P, Borbely AA. Low-frequency (< 1 Hz) oscillations in the human sleep electroencephalogram. Neuroscience 1997;81:213-22.
12. Massimini M, Huber R, Ferrarelli F, Hill S, Tononi G. The sleep slow oscillation as a traveling wave. J Neurosci 2004;24:6862-70.
13. Steriade M. Grouping of brain rhythms in corticothalamic systems. Neuroscience 2006;137:1087-106.
14. Mölle M, Marshall L, Gais S, Born J. Grouping of spindle activity during slow oscillations in human non-rapid eye movement sleep. J Neurosci 2002;22:10941-7.
15. Crunelli V, Hughes SW. The slow (< 1 Hz) rhythm of non-REM sleep: a dialogue between three cardinal oscillators. Nat Neurosci 2010;13:9-17.
16. Contreras D, Steriade M. Cellular basis of EEG slow rhythms: a study of dynamic corticothalamic relationships. J Neurosci 1995;15:604-22.
17. Destexhe A, Contreras D, Steriade M. Spatiotemporal analysis of local field potentials and unit discharges in cat cerebral cortex during natural wake and sleep states. J Neurosci 1999;19:4595-608.

18. Steriade M, Amzica F, Contreras D. Synchronization of fast (30-40 Hz) spontaneous cortical rhythms during brain activation. J Neurosci 1996;16:392-417.
19. Mölle M, Eschenko O, Gais S, Sara SJ, Born J. The influence of learning on sleep slow oscillations and associated spindles and ripples in humans and rats. Eur J Neurosci 2009;29:1071-81.
20. Mölle M, Yeshenko O, Marshall L, Sara SJ, Born J. Hippocampal sharp wave-ripples linked to slow oscillations in rat slow wave sleep. J Neurophysiol 2006;96:62-70.
21. Sejnowski TJ, Destexhe A. Why do we sleep? Brain Res 2000;886:208-23.
22. Werk CM, Harbour VL, Chapman CA. Induction of long-term potentiation leads to increased reliability of evoked neocortical spindles in vivo. Neuroscience 2005;131:793-800.
23. Marshall L, Born J. The contribution of sleep to hippocampus-dependent memory consolidation. Trends Cogn Sci 2007;11:442-50.
24. De Gennaro L, Ferrara M. Sleep spindles: an overview. Sleep Med Rev 2003;7:423-40.
25. Anderer P, Klosch G, Gruber G, et al. Low-resolution brain electromagnetic tomography revealed simultaneously active frontal and parietal sleep spindle sources in the human cortex. Neuroscience 2001;103:581-92.
26. Terrier G, Gottesmann CL. Study of cortical spindles during sleep in the rat. Brain Res Bull 1978;3:701-6.
27. Schabus M, Dang-Vu TT, Albouy G, et al. Hemodynamic cerebral correlates of sleep spindles during human non-rapid eye movement sleep. Proc Natl Acad Sci U S A 2007;104:13164-9.
28. Doran SM. The dynamic topography of individual sleep spindles. Sleep Res Online 2003;5:133-9.
29. Rechtschaffen A, Kales A. A manual of standardized terminology, techniques and scoring system for sleep stages of human subjects. Bethesda, MD: US Department of Health, Education and Welfare, 1968.
30. Huber R, Ghilardi MF, Massimini M, Tononi G. Local sleep and learning. Nature 2004;430:78-81.
31. Timofeev I, Bazhenov M. Mechanisms and biological role of thalamocortical oscillations. In: Columbus FH, ed. Trends in chronobiology research. New York: Nova Science Publishers, 2005:1-47.
32. Contreras D, Timofeev I, Steriade M. Mechanisms of long-lasting hyperpolarizations underlying slow sleep oscillations in cat corticothalamic networks. J Physiol 1996;494:251-64.
33. Bazhenov M, Timofeev I, Steriade M, Sejnowski TJ. Model of thalamocortical slow wave sleep oscillations and transitions to activated States. J Neurosci 2002;22:8691-704.
34. Hill S, Tononi G. Modeling sleep and wakefulness in the thalamocortical system. J Neurophysiol 2005;93:1671-98.
35. Destexhe A, Hughes SW, Rudolph M, Crunelli V. Are corticothalamic ‚up' states fragments of wakefulness? Trends Neurosci 2007;30:334-42.
36. Lüthi A, McCormick DA. Periodicity of thalamic synchronized oscillations: the role of Ca2+-mediated upregulation of Ih. Neuron 1998;20:553-63.
37. Schabus M, Gruber G, Parapatics S, et al. Sleep spindles and their significance for declarative memory consolidation. Sleep 2004;27:1479-85.
38. Fogel SM, Smith CT. Learning-dependent changes in sleep spindles and Stage 2 sleep. J Sleep Res 2006;15:250-5.
39. Nishida M, Walker MP. Daytime naps, motor memory consolidation and regionally specific sleep spindles. PLoS One 2007;2:e341.
40. Clemens Z, Fabo D, Halasz P. Overnight verbal memory retention correlates with the number of sleep spindles. Neuroscience 2005;132:529-35.
41. Clemens Z, Fabo D, Halasz P. Twenty-four hours retention of visuospatial memory correlates with the number of parietal sleep spindles. Neurosci Lett 2006;403:52-6.
42. Peters KR, Ray L, Smith V, Smith C. Changes in the density of stage 2 sleep spindles following motor learning in young and older adults. J Sleep Res 2008;17:23-33.
43. Siapas AG, Wilson MA. Coordinated interactions between hippocampal ripples and cortical spindles during slow wave sleep. Neuron 1998;21:1123-8.
44. Wierzynski CM, Lubenov EV, Gu M, Siapas AG. State-dependent spike-timing relationships between hippocampal and prefrontal circuits during sleep. Neuron 2009;61:587-96.
45. Gais S, Albouy G, Boly M, et al. Sleep transforms the cerebral trace of declarative memories. Proc Natl Acad Sci U S A 2007;104:18778-83.
46. Takashima A, Petersson KM, Rutters F, et al. Declarative memory consolidation in humans: a prospective functional magnetic resonance imaging study. Proc Natl Acad Sci U S A 2006;103:756-61.
47. Frankland PW, Bontempi B. The organization of recent and remote memories. Nat Rev Neurosci 2005;6:119-30.

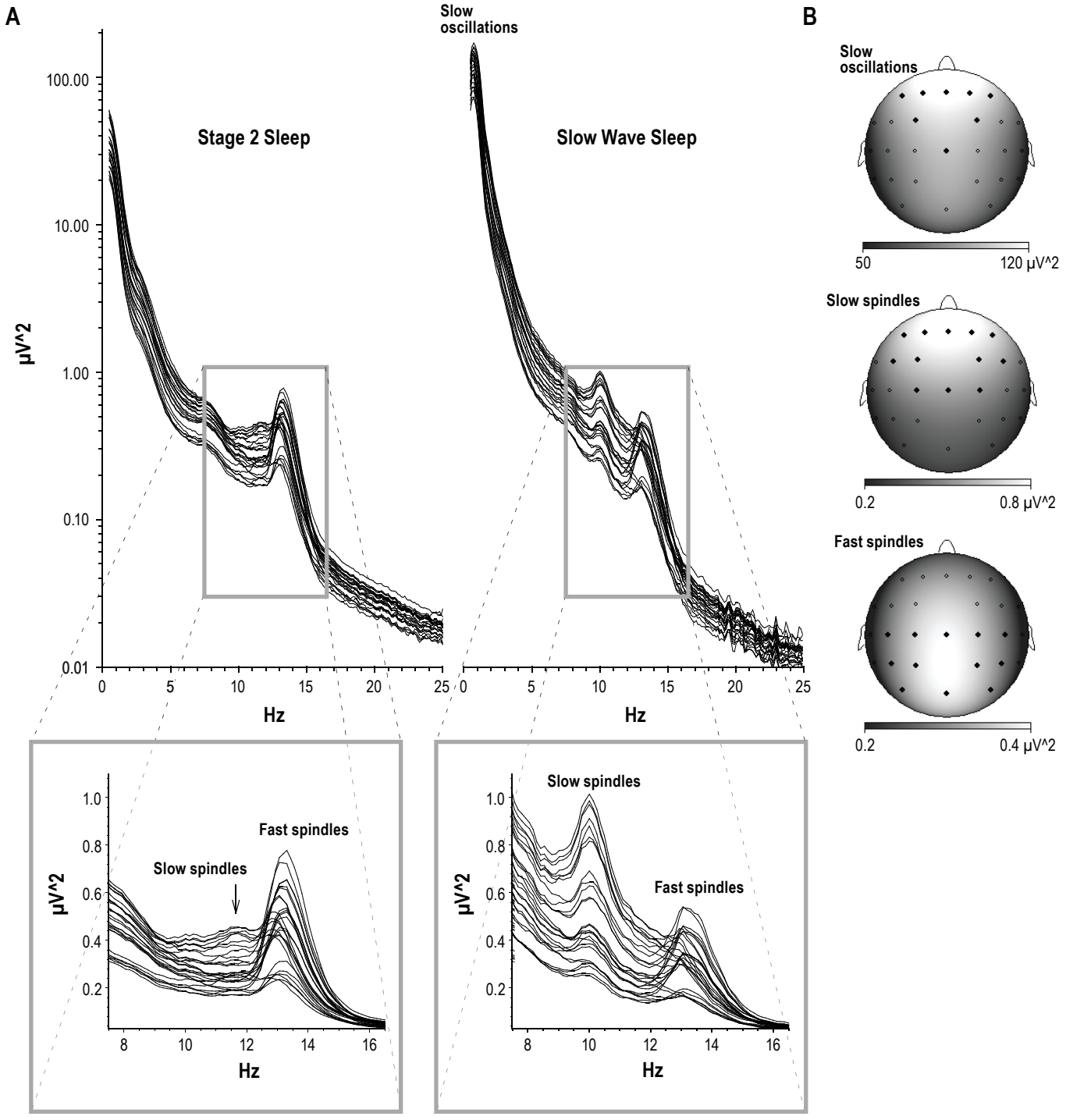

Figure S1—EEG power during NonREM sleep. **(A)** Comparison of EEG power during stage 2 sleep and SWS. Average spectra were calculated across the whole night for all 27 EEG channels. Insets show enhanced views of spindle activity. Note, although there are clear peaks for both, slow and fast spindle activity during SWS, only fast spindle activity shows a clear peak during stage 2 sleep. Note also distinctly higher power in the SO frequency band (0.5 - 1.3 Hz) during SWS than stage 2 sleep. **(B)** Maps indicating topography of power for the SO and the slow and fast spindle frequency ranges during SWS. Bold black dots indicate electrode positions of channels chosen for SO and slow and fast spindle detection.

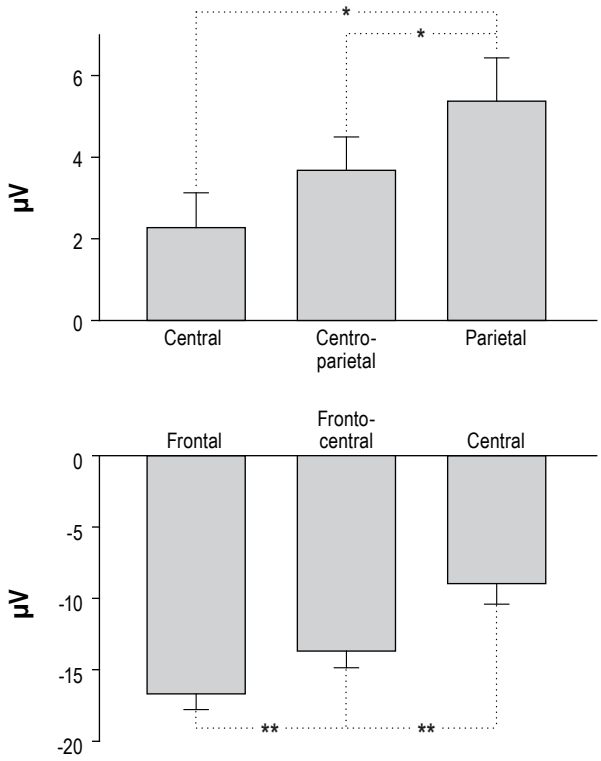

Figure S2—Potential shifts underlying fast spindles and slow spindles. Mean (± SEM) slow potential shifts underlying (top) fast spindles at central, centro-parietal and parietal electrodes and (bottom) slow spindles at frontal, fronto-central and central electrodes. Asterisks indicate significant differences between topographies in positive and negative slow potential shifts, respectively (**P < 0.01, *P < 0.05).

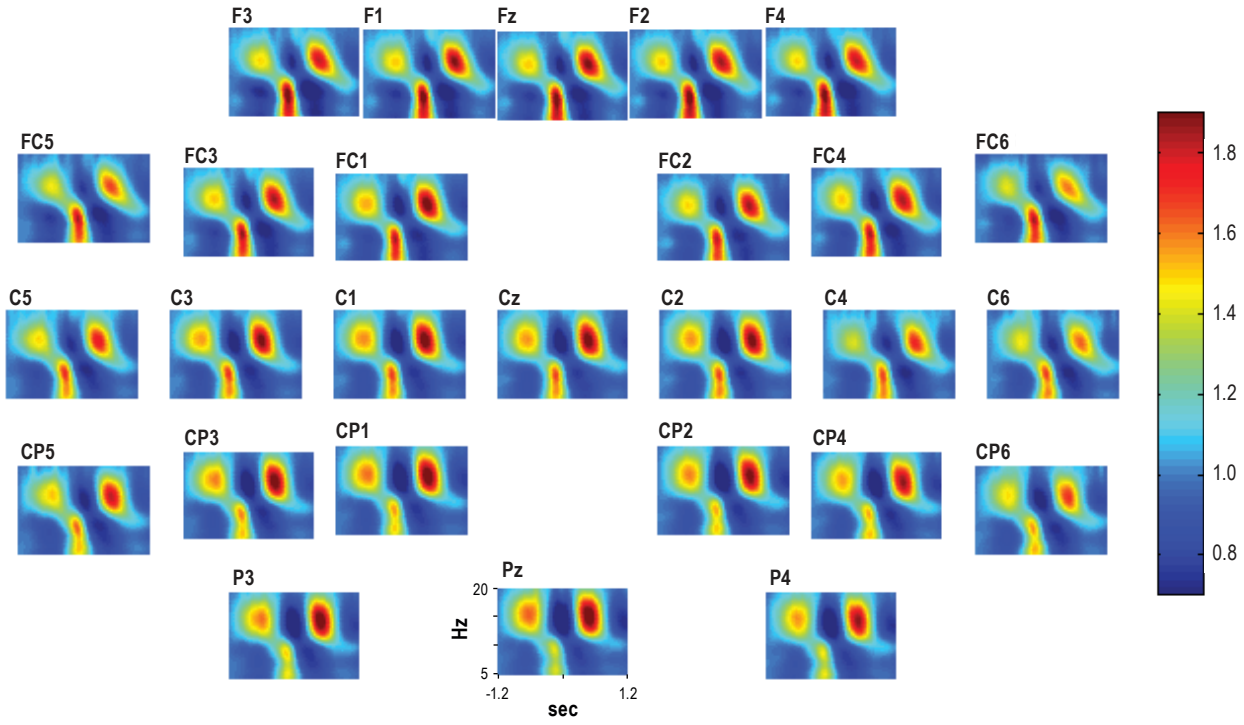

Figure S3—Time-frequency plots of wavelet-power during SOs. Time-frequency plots of wavelet-power for frequencies of 5-20 Hz in a time window of ± 1.2 sec around the negative peak of the SO (t = 0). Note, strongest modulation of fast spindle activity in the middle centro-parietal channels, and of slow spindle activity in the frontal channels, i.e., the respective sites of maximum spindle power.

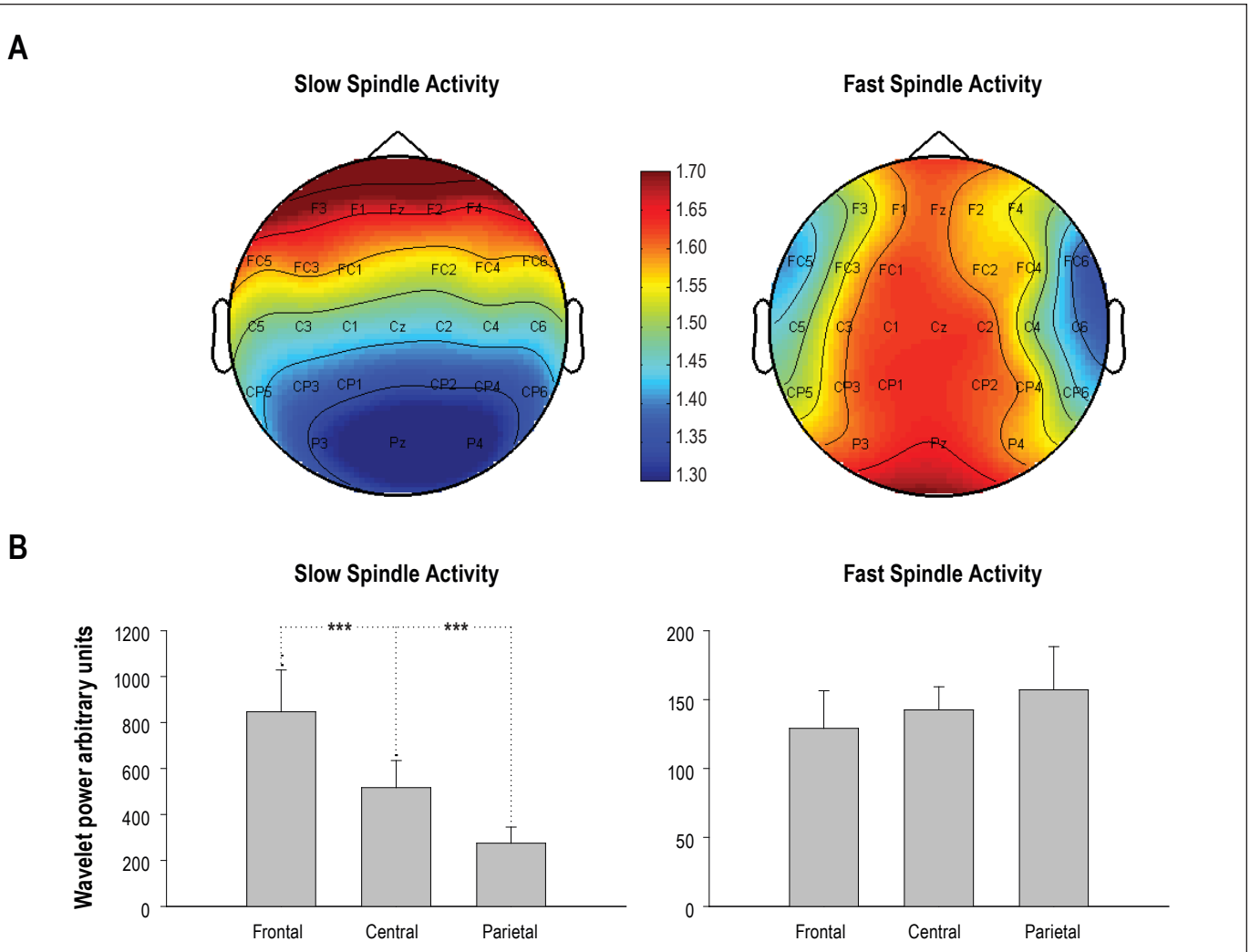

Figure S4—Scalp distributions of maximal spindle wavelet-power. **(A)** Scalp distributions of maximal slow (7-10 Hz, left) spindle wavelet-power (mean during the -0.2 to 0 sec-interval with reference to the negative SO peak) and of maximal fast (13-17 Hz, right) spindle wavelet-power (mean during 0.4 to 0.6 sec-interval). **(B)** Mean wavelet-power of slow (left) and fast (right) spindle activity in frontal (F3, Fz, F4), central (C3, Cz, C4) and parietal (P3, Pz, P4) electrodes. Asterisks indicate significant ($P < 0.001$) differences between electrode sites.

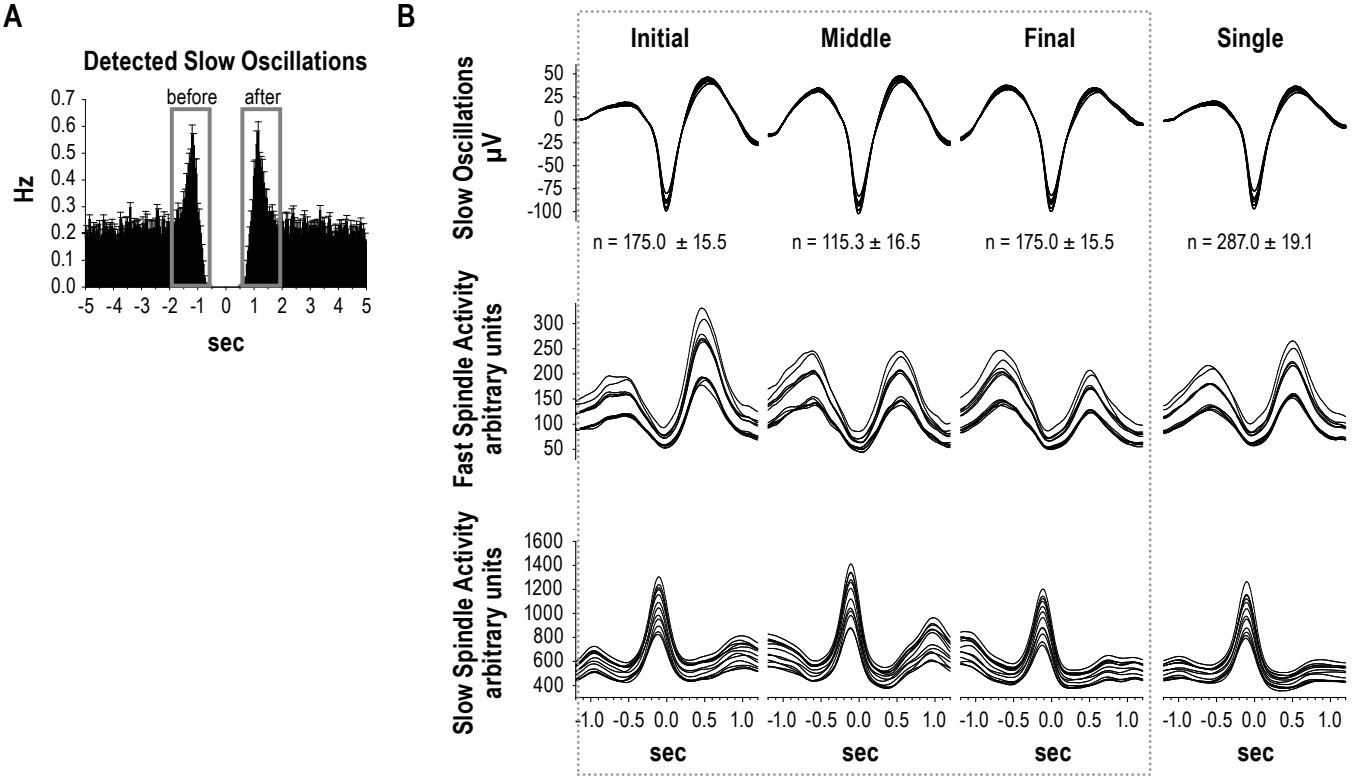

Figure S5—Analyses of sequences of slow oscillations. **(A)** Auto-event correlation histogram of all detected SOs in an 'average' channel (calculated by averaging the potentials of the 8 fronto-central channels of interest). Gray rectangles indicate time windows of increased probability of another SO preceding and/or following the actual SO. **(B)** Averages of the original EEG (upper panels) and the wavelet-power for slow (7-10 Hz) and fast (13-17 Hz) spindle activity during SOs that were or were not followed and/or preceded by another SO. Averaging of SOs was performed on the original unfiltered signal in the 8 fronto-central channels of interest. Fast spindle wavelet power is averaged for the 12 centro-parietal recording channels of interest, slow spindle wavelet power for the 12 fronto-central channels of interest. (Averages were calculated across all detected SOs and 11 subjects.) 'Initial', 'Middle', 'Final' indicate position of target SO in a sequence of (2-5) succeeding SOs; 'Single' – SO not occurring in a sequence.